Synthesis of carbon nanotubes and graphene for photonics applications
E. Einarsson and S. Maruyama, The University of Tokyo, Japan

Dr. E. Einarsson and Prof. S. Maruyama*
Department of Mechanical Engineering
The University of Tokyo
7-3-1 Hongo, Bunkyo-ku
Tokyo 113-8656
Japan

Email: maruyama@photon.t.u-tokyo.ac.jp

List of section headings:

Abstract:
This chapter provides an overview of methods used to synthesize single-walled carbon nanotubes (SWNTs) and graphene. Synthesis methods of commercially available SWNTs are reviewed first, followed by common in-house methods. Historically important approaches are discussed, but the focus is primarily on chemical vapor deposition (CVD). The first part ends with some discussion on how SWNTs can be tailored to photonics applications at the synthesis stage. Primary routes for graphene synthesis are described next, in addition to a bit of background regarding the relatively recent discovery of this two-dimensional material. Exfoliation of bulk graphite into single-layer graphene is described first, followed by synthesis routes involving reduction of graphene oxide and epitaxial growth from carbides. The chapter ends with an overview of CVD synthesis of graphene on metal substrates.

Key words: single-walled carbon nanotubes; graphene; nanotube synthesis; graphene synthesis; chemical vapor deposition

2.1 Introduction

In this chapter we describe the most common methods for synthesizing single-walled carbon nanotubes (SWNTs) and graphene. As discussed in the previous chapter, the physical properties of both SWNTs and graphene are largely determined by their structure, thus should be independent of synthesis method. However – particularly for nanotubes – this is not the case. Not only does chirality determine the properties of the SWNT, but many other factors such as environment, morphology, and presence of defects can also influence SWNT properties. Basic properties of graphene, such as electron mobility, are also strongly influenced by the environment, thus control over external influences is a critical issue. Numerous synthesis methods have emerged over the years, each having different merits and demerits. Some of these methods will be introduced and described here, but this will not be a thorough review of the subject. References are not intended to be comprehensive, but only highlight the first and/or highly influential works on the topic. We note that it is common to refer to a material by the way in which it was synthesized, such as HiPco nanotubes or CVD graphene. Lastly, due to their limited use in photonics – and for the sake of brevity – we omit any discussion on the synthesis of multi-walled carbon nanotubes.

2.2 Synthesis of single-walled carbon nanotubes (SWNTs)

Methods for synthesizing SWNTs can be roughly categorized into high temperature (above 2000 °C) and moderate temperature (between 500 and 1500 °C) approaches. In high temperature approaches, SWNTs condense during the cooling phase of a hot plasma of sublimated carbon. Such a plasma is typically generated by discharging a powerful electric arc between two graphite electrodes or by ablating a graphite target using an intense laser pulse. The former is known as the arc-discharge method, and had been used for fullerene synthesis (Krätschmer *et al.*, 1990) before leading to the discovery of SWNTs in 1993 (Iijima and Ichihashi, 1993; Bethune *et al.*, 1993). A schematic of an arc-discharge apparatus is shown in Fig. 2.1. The latter method is known by various names, including laser ablation, laser furnace, and laser oven. This method is also a descendant of fullerene research, as it was modified for SWNT synthesis by Richard Smalley (Guo *et al.*, 1995) shortly before he was awarded the Nobel Prize in Chemistry for the co-discovery of C_{60} (Kroto *et al.*, 1985). In the laser oven method, a graphite target is placed inside an electric furnace, as shown in Fig. 2.2. The cooling rate is controlled by keeping the reaction chamber at a moderately high temperature (above 800 °C). As is the case with fullerene synthesis, the cooling rate of the carbon plasma is critical to forming quality SWNTs, and changing the furnace temperature to adjust the cooling rate has been found to influence the mean diameter of the resulting SWNTs (Bandow *et al.*, 1998).

In both of these high temperature methods, the presence of a small amount (a few atomic per cent) of transition metal in the anode (Bethune *et al.*, 1993; Journet *et al.*, 1997) or in the target (Guo *et al.*, 1995; Thess *et al.*, 1996) is necessary for the formation of SWNTs. Nickel was initially regarded as the metal best suited for SWNT synthesis, but bimetallic mixtures such as Ni/Y for arc-discharge (Shi *et al.*, 1999) and Ni/Co or Rh/Pd for laser ablation (Kataura *et al.*, 2000) later showed to increase the nanotube yield. Laser ablation generally results in higher SWNT yield and offers better control over synthesis parameters than the arc-discharge method, but the prohibitive cost of the requisite high power laser makes this method less popular than arc-discharge or more economical

alternatives.

High temperature synthesis methods generally produce SWNTs with excellent crystallinity, but due to the extreme conditions during synthesis and lack of substrate for catalyst support, they offer little or no control over SWNT location or orientation. Catalytic chemical vapor deposition (CVD) offers such control, thus is an attractive alternative to high-temperature methods. Not only does CVD allow for the use of patterned substrates, but the method is also easily scalable, as evidenced by its widespread use in the semiconductor industry. CVD is also a more economical alternative than the aforementioned high temperature approaches because it requires neither high-power lasers nor high vacuum, and systems can even be operated at atmospheric pressure. Due to these advantages, CVD has become the synthesis method of choice for the nanotube community.

The term CVD encompasses a wide range of methods that share the same underlying principle. In the CVD process, SWNTs are synthesized via a chemical reaction between a carbon-containing precursor and a catalyst nanoparticle (Dai *et al.*, CPL 1996). The reaction typically occurs at temperatures between 500 and 1000 °C, and the catalyst nanoparticles are typically transition metals. A schematic of a substrate-supported CVD system is shown in Fig. 2.3. Unsupported 'floating catalyst' or fluidized bed approaches are also common, in which a metal-containing precursor such as $Fe(CO)_5$ (iron pentacarbonyl) or $Fe(C_5H_5)_2$ (ferrocene) is injected along with the carbon feedstock gas. The catalyst nanoparticles form *in situ* via decomposition of the metal-containing precursor, and subsequently react with the available carbon to form SWNTs before the gas flow carries them out of the high-temperature region (Satishkumar *et al.*, 1998; Cheng *et al.*, 1998). Using various CVD approaches, SWNTs have been synthesized from a number of feedstock gases including carbon monoxide (Dai *et al.*, 1996; Hafner *et al.*, 1998), simple hydrocarbons (Kong *et al.*, 1998a; Cassell *et al.*, 1999; Hafner *et al.*, 1998), and alcohol (Maruyama *et al.*, 2002).

Despite its widespread use in the arc-discharge and laser oven method, Ni has proved to be a relatively poor catalyst for SWNT synthesis by CVD. The reason for this is not entirely clear, but Fe, Co, and their compounds have thus far proved to be much more effective. The majority of CVD methods also utilize MgO, Al_2O_3, or zeolite as a catalyst support. Synthesis of SWNTs from catalyst nanoparticles directly deposited on quartz was demonstrated by Murakami and co-workers (2003), but in most cases of substrate-supported growth, catalyst support layers are still employed to enhance SWNT yield.

Although CVD-synthesized carbon fibers have been commercially available since before the discovery of SWNTs, synthesis of SWNTs has proved much more difficult than simply scaling down the carbon fiber process. In order to realize SWNT generation, arc-discharge, laser-over, and new CVD methods needed to be developed. After two decades of research into SWNT synthesis, a number of well-developed synthesis methods have emerged. As a result, the cost of SWNTs has dropped to the point where purchase of commercially available SWNTs is now an economically feasible option. Interestingly, however, recent CVD methods still resemble the decades-old process used for carbon fiber generation (Endo, 1988). There have been considerable advancements,

however, in preparation of nanoscale metal catalyst particles and control of the growth reaction. Researchers developing photonics applications are perhaps more likely to purchase SWNTs than to synthesize their own, so we describe next the major types of commercially available SWNTs.

2.2.1 Commercially available SWNTs

A quick Internet search will return a growing list of distributors supplying SWNTs produced by some of the methods described above, but here we limit our discussion to a couple of widely available and historically important processes.

The most thoroughly studied SWNT material has been produced by high-pressure disproportionation of carbon monoxide, or the HiPco® process (Nikolaev *et al.*, 1999), which was developed by Richard E. Smalley's group at Rice University. In this process, gas-phase carbon monoxide and iron pentacarbonyl, $Fe(CO)_5$, are combined under very high pressure (~30 atm) and temperatures between 900 and 1100 °C (Bronikowski *et al.*, 2001). The $Fe(CO)_5$ decomposes to form iron clusters, which nucleate SWNTs. Selectivity to SWNTs by the HiPco method is not perfect, so the as-produced material contains various carbon nanostructures as well as a considerable amount of metal catalyst. Hence, the SWNTs are generally purified by chemical post-processing, but the as-produced material is also available. HiPco SWNTs have a somewhat narrow diameter distribution, ranging from 0.8 to 1.2 nm. Carbon Nanotechnologies Inc. (CNI) brought the HiPco process to market in the year 2000; it was later acquired by Unidym, the current producer of HiPco nanotubes. The HiPco process was the first method capable of producing SWNTs on a gram-per-day scale. From a research standpoint, quite a lot can be done with a gram of SWNTs, and HiPco nanotubes were made available to researchers throughout the nanotube community. This significantly accelerated the pace of nanotube research by allowing for direct comparison of results from laboratories around the globe. As a result, HiPco nanotubes became the *de facto* standard against which characterization methods and other SWNT properties were compared.

The second most widely available commercial SWNT is known as CoMoCAT®. Similar to HiPco, CoMoCAT is based on the CO disproportionation reaction. Different to HiPco, however, the CoMoCAT process utilizes a bimetallic cobalt-molybdenum catalyst, and the reaction takes place at a somewhat lower pressure (~5 atm). Elevated pressure is still necessary, however, to drive the CO disproportionation reaction away from equilibrium to produce solid carbon. CoMoCAT nanotubes have a narrow diameter distribution, with a mean diameter of only 0.8 nm and a high selectivity for the chirality (6,5). The CoMoCAT process was originally developed by Daniel Resasco's group at the University of Oklahoma (Kitiyanan *et al*., 2000), and was later incorporated into the business venture SouthWest NanoTechnologies, Inc. (SWeNT).

A third well known method is alcohol catalytic CVD (ACCVD, Maruyama *et al*., 2002). Although SWNTs synthesized by the ACCVD method are commercially available through the University of Tokyo, this fact is not widely known so we introduce the ACCVD method in the following section addressing in-house methods.

2.2.2 In-house SWNT synthesis methods

Since the optical transition energies of SWNTs are inversely proportional to their

diameter (Kataura *et al.*, 1999), small-diameter SWNTs such as CoMoCAT may be suitable for some optical applications. For other uses however, attributes such as broad diameter distribution, controlled morphology, or high-purity of pristine material may be desirable. Since there is little option to custom-order commercially available SWNTs, laboratory-scale synthesis methods are still under active development.

The majority of in-house synthesis methods are based on CVD. Due to the flexibility of the CVD process, there is a huge parameter space to explore, including myriad catalysts, substrates, carbon precursors, and pressure and temperature ranges. Among these methods, ACCVD is one of the simplest, and is known to produce very clean, high-quality SWNTs (Fig. 2.4). The low cost and ease of handling ethanol makes ACCVD an attractive option, particularly when combined with wet catalyst preparation methods that do not require expensive vacuum equipment. Two approaches often used with ACCVD involve loading catalyst nanoparticles onto support materials either by impregnating the nanoparticles into zeolite (Mukhopadhyay *et al.*, 1999, Maruyama *et al.*, 2002) or by dip-coating onto flat substrates (Murakami *et al.*, 2003). When synthesized on zeolite, SWNTs produced by ACCVD have a diameter distribution slightly narrower than HiPco, but when grown on Si or quartz substrates they have a broad diameter distribution centered on 1.9 nm. Although the diameter is larger in the substrate-supported case, the produced SWNTs are vertically aligned (Murakami *et al.*, 2004). Catalyst conditions suitable to SWNT synthesis are considerably different to those resulting in growth of multi-walled nanotubes (Kakehi *et al.*, 2008), and alcohol has shown to have a high selectivity toward producing SWNTs. The absolute yield, however, is somewhat lower than other methods.

Perhaps the most well known non-commercial method is the so-called ‘super-growth’, or water-assisted CVD method (Hata *et al*., 2004). Ethylene or acetylene precursors are very widely used to grow nanotubes from Fe catalyst nanoparticles, which form at high temperature from an alumina-supported Fe thin-film. The water-assisted CVD method adds to this recipe a small but well-controlled amount of water (~140 ppm). This small addition was found to significantly enhance both catalyst activity and catalyst lifetime (Futaba *et al*., 2005; Hasegawa and Noda, 2011), resulting in very high yield of substrate-supported SWNTs (Fig. 2.5). Various substrates have been used with this method, including Si wafers, quartz plates, and metal foils (Hiraoka *et al*., 2006), but exceptionally precise control and monitoring of the partial pressures of the high-purity precursors is critical to successfully reproducing this method (Noda *et al.*, 2007). The mean diameter of SWNTs synthesized by water-assisted CVD is a rather large 3.0 nm, and some double-walled nanotubes are also present (Futaba *et al*., 2006a). The importance of oxygen in the CVD process was brought to light by the ACCVD method, where oxygen is present in the alcohol’s hydroxyl group. The water-assisted CVD method further revealed the importance of oxygen, in this case present as water. The critical role of oxygen in SWNT synthesis was later clarified in a comprehensive follow-up study by Futaba and coworkers (2009).

2.3 SWNT synthesis for photonic applications

Due to their quasi-one-dimensional structure, many SWNT properties are highly anisotropic. Making use of this anisotropy requires that the SWNTs be preferentially oriented on a macroscopic scale, but SWNTs tend to grow in random directions, forming

a bundled mat of nanotubes. Certain substrates or synthesis conditions, however, can help tame this naturally disordered system.

2.3.1 Horizontal alignment

Some early success in achieving horizontally aligned growth was obtained by applying an external electric field (Y.G. Zhang *et al.*, 2001; Joselevich and Lieber, 2002), which exploited the highly anisotropic polarizability of SWNTs (Benedict *et al*., 1995). Aligned growth was also realized by using the flow of the feedstock gas itself (Huang *et al.*, JACS, 2003), a method that has produced cm-long SWNTs (Zhou *et al*., 2006). The nanotube density achieved by these methods, however, is generally very low. Ismach and coworkers (2005) demonstrated the strong influence a substrate could exert on a SWNT's orientation by discovering that SWNTs grew along step edges on the surface of slightly mis-cut quartz crystal. After investigating a variety of crystal surfaces, high-density aligned growth was found to occur on sapphire (Han *et al*., 2005; Ago *et al*., 2005) as well as on ST-cut crystal quartz (Kocabas *et al.*, 2005). The cause of alignment on sapphire was quickly obvious, but the latter remained a puzzle for many years because of the inhomogeneity in the ST-cut surface. It was recently shown that the crystal quartz R-plane is responsible for the alignment (Chiashi *et al.*, 2012), and the mechanism is similar to that of aligned growth on sapphire. Some aligned SWNTs grown by these methods are shown in Fig. 2.6. Highly aligned SWNTs with average linear densities exceeding 20 SWNTs/μm have been achieved (Hong *et al*., 2010).

2.3.2 Vertical alignment

Orientation perpendicular to the substrate surface is another desirable morphology. This was first reported in early 2004 (Murakami *et al*., 2004), and was followed shortly thereafter by several other reports using numerous CVD methods. Synthesis of vertically aligned SWNTs (VA-SWNTs) is now a common practice, and various morphologies can be obtained by patterning the deposited catalyst. One example of this is shown in Fig. 2.7, where periodic VA-SWNT walls were grown and then knocked over in order to obtain high-density horizontally aligned SWNTs (Pint *et al*., 2008; Hayamizu *et al.*, 2008).

The low volume density (3–5 wt.%) of the VA-SWNT array is attractive for a number of reasons. The sparse structure means the array has a very high specific surface area (>1000 m^2/g), yet can be compressed while preserving or improving the alignment (Futaba *et al*., 2006b). Some applications proposed for such materials are catalyst support materials and electrodes for super-capacitors or fuel cells. From an electrical/optical standpoint, it has been shown that the vertically aligned SWNT array is essentially a bulk material whose properties are determined by those of the constituent one-dimensional SWNTs (Kramberger *et al*., 2008). This is attributed to the low extent of bundling within the array (Einarsson *et al*., 2007), which preserves the unique properties of the SWNTs that arise from their one-dimensional structure.

VA-SWNT arrays also offer the advantage of being transferable. Millimeter-scale arrays, such as that shown in Fig. 2.5a, can be removed from their growth substrate simply by picking them off with tweezers or scraping them off using a razor blade (Hata *et al*., 2004). VA-SWNT arrays as short as 1 μm can be removed from the underlying substrate by submerging the substrate into hot water (Murakami and Maruyama, 2006), provided the arrays are hydrophobic. The floating array can then be transferred onto any arbitrary

surface – including thin optical fibers (Song *et al*., 2007) – whilst preserving the alignment. Additional methods exist that involve, for example, chemically etching away the substrate to release the vertically aligned SWNT array (Zhang *et al*., 2005).

2.3.3 Tailoring diameter and chirality distribution

Despite having some control over the SWNT morphology on a large scale, all current synthesis methods still produce SWNTs with various diameter ranges (Fig. 2.8) and contain a distribution of chiralities. The mean SWNT diameter can often be tuned by modifying the catalyst amounts and relative concentrations (e.g., Xiang *et al*., 2012; Thurakitseree *et al.*, 2012a). In the case of ACCVD, the mean diameter of vertically aligned SWNTs could be reduced to less than 1 nm by the addition of a few per cent acetonitrile (CH_3CN) into the ethanol feedstock (Thurakitseree *et al.*, 2012b). Attempts at reducing the number of chiralities present in a sample usually are based on reducing the average diameter, but chirality-selective growth has seen limited success. However, a number of post-processing methods have been developed by which single-chirality SWNTs can be extracted. A recent method based on gel chromatography (Liu *et al*., 2011) is very promising because it exhibits tremendous potential for large-scale separation. However, the most common method by which SWNTs are separated is density gradient ultracentrifugation (DGU). DGU relies on wrapping the SWNTs with either a surfactant (Arnold *et al*., 2005) or DNA (Zheng *et al*., 2003). This wrapping enhances the minuscule density differences of SWNTs having slightly different diameters. DGU is capable of separating the SWNTs, but the difficulty associated with removing these wrapping agents limits the potential uses of the separated SWNTs. An example of single-chirality extraction is shown in Fig. 2.9. DGU has also seen widespread use for separating SWNTs based on electronic character (Arnold *et al*., 2006). DNA wrapping is perhaps the most effective method to extract single-chirality SWNTs (Tu *et al*., 2009), but the yield is extremely low and the procedure is prohibitively expensive.

While a number of separation methods have been developed, the problem of how to directly synthesize semiconducting, metallic, or SWNTs of the same chirality remains unsolved. There have been a number of reports on preferential synthesis of semiconducting (Y. Li *et al*., 2004; Qu *et al*., 2008) or metallic (Harutyunyan *et al*., 2009) SWNTs, but work continues in this area. A number of post-processing methods have also been reported, in which semiconducting or metallic nanotubes are selectively etched to obtain SWNTs with a dominant electronic character (G.Y. Zhang *et al.*, 2006; Miyata *et al*., 2006). Wet post-processing methods have proved quite effective at separating metallic and semiconducting SWNTs (not chirality selective), and type-separated SWNTs can be purchased from NanoIntegris Inc., and Meijo Nano Carbon Co., Ltd.

2.4 Graphene synthesis

Although the discovery of graphene involved some degree of serendipity, it did not come entirely out of the blue; the isolation of a single atomic layer of carbon had actually been pursued for some time. The use of ultra-thin graphite crystals as an ideal support membrane for high-resolution electron microscopy was suggested more than 50 years ago (Fernández-Morán, 1960), but researchers could not manage to obtain anything thinner than a few nanometers. In fact, despite decades of trying, a single graphene layer

had been so elusive that many assumed it was thermodynamically too unstable to actually exist, and would instead roll itself into a cylindrical or spherical structure (Kroto and McKay, 1988; Robertson *et al*., 1992). Although this explains fullerene formation, and is generally true in the absence of a supporting surface, we learned in 2004 that single graphene layers can indeed exist (Novoselov *et al.*, 2004).

2.4.1 Mechanical exfoliation of graphite

As described in the previous chapter, graphene is a planar, single atomic layer of sp^2-bonded carbon. Multiple layers of graphene stacked atop one another is the very common form of carbon known as graphite. Hence, it should come as no surprise that single-layer graphene was first obtained by exfoliating these layers from a bulk piece of graphite.

The Van der Waals interaction between two graphene layers corresponds to a force of approximately 2 eV mm^{-2}, which can be overcome by applying a normal force of approximately 300 nN to a 1 μm^2 piece of graphite (Y.B. Zhang *et al*., 2005). This weak force can easily be overcome simply by rubbing a piece of graphite against another surface, a phenomenon we observe every time we write or draw with a pencil. Many researchers attempted in this way – with varied degrees of success – to shear off a single layer of graphene. In 1999 The Ruoff group clearly demonstrated the potential of this approach to obtain a single layer (Fig. 2.10), but were ultimately unsuccessful (Lu *et al*., 1999). The Kim group attempted to improve upon Ruoff's attempt by essentially scaling down the pencil. They attached a tiny piece of graphite onto the tip of an atomic force microscope (AFM), in hopes that they could adjust the applied force to an appropriate magnitude that would cause the shearing of individual layers (Y.B. Zhang *et al*., 2005). This approach was also promising, but they were unable to obtain anything thinner than 10 nm. What was eventually successful, however, was conceptually an equally simple approach.

Anyone who has used or seen a demonstration of an AFM or scanning tunneling microscope (STM) is probably familiar with the hexagonal surface of highly oriented pyrolytic graphite (HOPG). In order to obtain a flat surface for clear imaging, the topmost layers of the HOPG sample are cleaved from the bulk by simply attaching a piece of adhesive tape and peeling it off. The freshly cleaved HOPG is then placed on the sample stage while the piece of tape is discarded. One day, a group of researchers at Manchester University turned their attention to the piece of tape and decided to see how far they could scale down the cleaving process.

Novoselov and co-workers fixed small 'mesas' of HOPG atop a glass substrate by embedding them in a photoresist. These graphite mesas were then made increasingly thin by repeatedly cleaving with adhesive tape. Eventually, single layers of graphene remained in the photoresist, and were released by dissolving the resist with acetone and rinsing with water. After capturing the floating graphite and graphene layers by dipping a silicon wafer into the solution, they were faced with the more difficult task of finding the atomically thin layers. Purely by chance, the researchers had captured the floating graphene using a silicon wafer coated with a 300 nm thick oxide layer; this turned out to be extremely fortunate.

Since the surface of the Si wafer was far too large an area to survey using scanning probe methods, and graphene is nearly invisible inside an electron microscope, the researchers' only choice was to manually search using an optical microscope. It turns out that at the wavelength where the human eye is most sensitive (550 nm), a single layer of graphene will provide maximum contrast when sitting atop a silicon wafer coated with an oxide layer either 90 or 300 nm thick (Blake *et al*., 2007). The reason is that the system forms a Fabry-Perot multilayer cavity, in which 'the oxide surface reflects a rainbow of colours, and the interference pattern produced by layers of graphene on the oxide provides a faint but visible contrast, much like the fringes in an oily puddle' (Geim and MacDonald, 2007). This contrast can be clearly seen in the optical image in Fig. 2.11. The serendipitous choice of substrate therefore meant single-layer graphene was first detected by the human eye.

The method described above (Novoselov *et al*., 2004) was subsequently simplified into what is now known as the 'Scotch™ tape method' or 'drawing method' (Novoselov *et al*., 2005). As its name implies, one cleaves the topmost layer from a piece of HOPG, and then cleaves that thin layer repeatedly using the same adhesive tape. Statistically, a 1 μm flake should be reduced to one atomic layer after cleaving a dozen times. The tape is then gently rubbed against a substrate suitable for locating graphene, i.e., a Si wafer coated with an oxide layer 90 or 300 nm thick. One then searches for the thinnest flakes using an optical microscope (a green filter facilitates the process). This simple method, which basically requires nothing more than a typical optical microscope and your favorite brand of sticky-tape, is capable of producing graphene flakes hundreds of square micrometers in size (Novoselov *et al*., 2005). Videos demonstrating the process are also readily available online.

2.4.2 Chemical exfoliation of graphite

Chemists had also been attempting to obtain individual graphene layers for many years, but of course doing so in solution. Their primary approach was to generate a reaction that would splinter a piece of graphite into its component atomic layers by intercalating a material in between the layers and then reacting the intercalant. The most common method is known as Hummers method (Hummers and Offeman, 1958), and involves intercalation of potassium permanganate into a graphite crystal. This process alone does not separate the individual graphene layers, but dramatically increases the interlayer spacing. One can then splinter apart the expanded graphite by heating it extremely rapidly, e.g., at more than 2000 ºC/min (Schniepp *et al.*, 2006; Stankovich *et al.*, 2007). This causes the intercalant to decompose, generating CO_2 at a rate faster than the gas can escape, and essentially blows the graphite apart. The product of chemical exfoliation methods such as Hummers method is not pristine graphene but a functionalized form known as graphene oxide (GO). An optical image of GO obtained by fluorescence quenching microscopy is shown in Fig. 2.12 (J.M. Kim *et al.*, 2010). In GO, most of the sp^2-bonded planar structure has been converted into an sp^3-bonded material. This step must somehow be undone by completely reducing the GO. Determining how to do this effectively is the goal of a very active research community, a review of which is beyond the scope of this chapter. We suggest the interested reader look for recent review articles on the subject, such as those by Park and Ruoff (2009), Eda and Chhowalla (2010), or Loh *et al*. (2011).

An alternate chemical method for obtaining graphene is by exfoliating and dispersing graphite in an organic solvent such as N-methyl-pyrrolidone, or NMP (Hernandez *et al*., 2008). This method may be of particular interest to those in the photonics community, as organic solvents such as NMP have been used for dispersing SWNTs without the need for surfactants (Furtado *et al.*, 2004). A similar approach has also been effectively used with carbon nanotubes and graphene to fabricate broadband optical limiters (Riggs *et al*., 2000; Lim *et al*., 2011). The graphene layers are not oxidized by this method thus should have fewer defects and be usable directly after deposition. Intercalation by an electron-donor such as potassium prior to dispersion charges the graphene sheets to the point that the charged graphite spontaneously delaminates when placed in NMP; no sonication required (Vallés *et al*., 2008).

Although generally defect-inducing and thus avoided, sonication can have its merits. As is the case with SWNT dispersions, ultrasonication of graphene dispersions can induce significant defects and even break up the material. Very aggressive sonication can thus be a means to obtain small fragments or ribbons of graphene (X.L. Li *et al.*, 2008), which become semiconducting if the nanoribbon has a width of less than ~20 nm (Nakada *et al.*, 1996). Some progress on 'unzipping' carbon nanotubes to obtain graphene nanoribbons has also been reported (Kosynkin *et al*., 2009; Jiao *et al*., 2009).

2.4.3 Epitaxial growth of graphene

Methods described in the previous two sections share one common drawback, and that is the difficulty in placing the obtained graphene in a specified location. One method by which graphene can be synthesized in precisely controlled locations is epitaxial growth of graphene directly from a carbide surface. In this approach, the carbide is heated to a temperature that is sufficiently high to evaporate the non-carbon atoms from the surface, leaving a pure carbon surface behind. Under appropriate conditions, the remaining carbon atoms reorganize themselves into graphene. It has been found that this thermal process considerably roughens the surface when performed in vacuum, typically resulting in multiple layers of poorly formed graphene (Hass *et al*., 2008). Under an argon atmosphere, however, well-formed single-layer graphene can be formed on a Si-terminated SiC surface. Sublimation of the Si from the surface requires temperatures above 1500 ºC, but the resulting graphene is of very high quality and is well suited for wafer-scale processing (Emtsev *et al*., 2009). Patterning the SiC surface also allows one to control the size, shape, and location of graphene with the precision necessary to fabricate graphene integrated circuits (Berger *et al.*, 2006, Sprinkle *et al.*, 2010, Lin *et al.*, 2011), as shown in Fig. 2.13. Despite the advantages of epitaxial growth, the scalability is poor due to the high processing temperature and cost of SiC wafers. As was the case with SWNTs, researchers have thus changed their focus to the less costly, more scalable CVD method.

2.4.4 Graphene synthesis by chemical vapor deposition

By building on a decade's worth of literature on nanotube synthesis, graphene synthesis by CVD has progressed very rapidly. It turns out the choice of precursors is much less restrictive than for SWNTs, as graphene has been synthesized from everything from methane to ordinary table sugar (Sun *et al.*, 2010). Regardless, methane is very widely used and is well suited for producing high-quality single-layer graphene (K.S. Kim *et al.*, 2009; X.S. Li *et al*., 2009a). A wide range of transition metal substrates can also be used,

with reports of growth on iridium (Coraux *et al.*, 2008), ruthenium (Sutter *et al.*, 2008), platinum (Sutter *et al.*, 2009), copper (X.S. Li *et al.*, 2009a), nickel (K.S. Kim *et al.*, 2009), and palladium (Murata *et al.*, 2010). Among these, Ni and Cu have been the most thoroughly studied, and it turns out the graphene growth mechanism on these metals is quite different. The following two mechanisms have been identified by isotopically labeling the carbon precursors used during CVD and then evaluating the Raman spectra of the resulting graphene (X.S. Li *et al.*, 2009b).

Carbon has very limited solubility in copper, so it is believed that carbon supplied during CVD primarily adsorbs onto the Cu surface and assembles into a planar sp^2 network. This exclusively surface process suggests the growth on Cu is self-limiting, with excess carbon having little influence on the final product. On the other hand, carbon has an appreciable solubility in nickel, thus carbon supplied during CVD can dissolve into the bulk Ni. When the temperature begins to decrease from the growth temperature (typically 900 ºC or higher) a portion of the dissolved carbon segregates out of the bulk, forming a graphitic layer on Ni(111) free surfaces (Odahara *et al.*, 2011; Takahashi *et al.*, 2012). As the temperature decreases further, however, the carbon that is still dissolved in the Ni will precipitate out of the bulk and form additional layers of graphitic carbon on the surface (Shelton *et al.*, 1974; Eizenberg *et al.*, 1979). Terminating the CVD process with a fast cooling (quenching) step has been widely used to limit the precipitation and obtain single-layer or few-layer graphene on nickel (K.S. Kim *et al.*, 2009), but is not necessary when using copper substrates. As segregation only occurs on Ni(111) surfaces, the use of single-crystal substrates becomes necessary for synthesis of uniform, high-quality graphene on nickel (Y. Zhang *et al.*, 2010). In addition to surface precipitation, dissolved carbon can also exit the bulk by emerging from step edges present on the Ni surface (Weatherup *et al.*, 2011). The carbon can then extend out across the surface, forming an sp^2 network (Gamo *et al.*, 1997). This process is illustrated in Fig. 2.14, and is reminiscent of earlier findings by the same group regarding nanotube wall formation (Hofmann *et al.*, 2007).

CVD-grown graphene can be easily patterned (Reina *et al.*, 2009), and various methods for post-CVD transfer of graphene have been reported (e.g., Reina *et al.*, 2009; K.S. Kim *et al.*, 2009; X.S. Li *et al.*, 2009a). The electrical properties of CVD-grown graphene are still inferior to those of graphene obtained by exfoliation methods, but the optical properties of CVD graphene can be uniform over large areas (Fig. 2.15). Roll-to-roll production of transparent electrodes using CVD-grown graphene has already been realized, demonstrating the scalability of CVD methods.

Raman spectroscopy has proved to be an invaluable tool for the study and characterization of graphene. The primary reason Raman spectroscopy is used to characterize graphene is that the 2D band (the overtone of the D band, also called G') is sensitive to the number of graphene layers (Ferrari *et al.*, 2006), as shown in Fig. 2.16. This allows one to distinguish single-layer graphene from multi-layer or even bi-layer graphene using a simple, nondestructive spectroscopic measurement. Furthermore, the D band feature, which arises from symmetry breaking often due to the presence of defects, has been found to come primarily from crystallite edges (Pimenta *et al.*, 2007). The ratio of the D band intensity to the G band intensity can thus be used to estimate the crystallite size (Cançado *et al.*, 2006).

Much has been learned about CVD synthesis of graphene, but one thing that has recently become clear is that the product is usually not the single atomic layer of carbon we imagine. In graphite, the graphene layers are stacked atop one another with some relative orientation. The lowest energy case is known as Bernal (or AB) stacking, and in this configuration the graphene unit cells are offset in such a way that the atoms in the upper layer are concentric with the hexagons of the layer below. Significant interlayer coupling in this configuration modifies the π electron dispersion relations near the *K* point in the Brillouin zone. This leads to additional double-resonance Raman scattering processes, which cause the 2D (G') Raman feature to become broader and asymmetric, allowing one to distinguish between single-layer and bi-layer graphene (Ferrari *et al.*, 2006; Castro Neto *et al.*, 2009). CVD-grown graphene often exhibits the simple, symmetric lineshape associated with single-layer graphene, but recent findings shows this may have been misleading.

When stacked graphene layers are offset from this AB configuration, a moiré pattern appears and the interlayer coupling weakens. This makes the Raman spectra of multi-layer graphene nearly indistinguishable from that of single-layer graphene (MacDonald and Bistritzer, 2011). However, a decreased Fermi velocity in such offset-stacked graphene should cause a slight shift in the position of the 2D Raman line (dos Santos *et al.*, 2007; Ni *et al.*, 2008). It turns out that many processes believed to have produced single-layer graphene had been incorrectly identified. Furthermore, when graphene is synthesized on SiC, the first one or more layers are strongly bound to the underlying SiC, thus do not exhibit the 2D lineshape associated with single-layer graphene (Hass *et al.*, 2008). Due to a strong carbon-nickel interaction, the bottom-most graphene layer grown on nickel is similarly Raman silent (Takahashi *et al.*, 2012). Interestingly, however, moiré patterns are generally not found for graphene grown on Cu substrates. This has been explained by copper's self-limiting surface-adsorption growth mechanism described above (X.S. Li *et al.*, 2009b). In light of this new information, the focus of the graphene synthesis community has recently shifted to obtaining not only true single-layer graphene, but also single-*crystal* graphene by CVD (X.S. Li *et al.*, 2011; Gao *et al.*, 2012, Yan *et al.*, 2012).

2.5 Summary and outlook

Synthesis of SWNTs has been thoroughly investigated over the past two decades. In the resulting body of scientific literature, much of the parameter space has been explored and we are now able to select suitable precursors, catalysts, and growth conditions to synthesize high-quality SWNTs in appreciable amounts. There are a number of methods available by which we can exert control over the properties or morphology of the synthesized nanotubes, but the challenges of precisely controlling diameter and chirality remain. Regardless of these challenges, the maturity of CVD as an affordable, reliable synthesis method has made SWNTs increasingly available. Further advances in diameter and chirality control will be of particular interest to the photonics community.

The scientific community has also made great strides in its ability to synthesize graphene, whether using novel or revisited approaches. The variety in synthesis methods – from simple tabletop procedures to large-scale wet-chemical processes – offers flexibility in choosing the appropriate method for a desired application. Mechanical exfoliation, for

example, generally provides graphene flakes with the best crystallinity and the largest domain size. Chemical reduction of graphene oxide, on the other hand, can produce uniform graphene over large areas. Precise patterns of graphene can also be grown directly on the face of SiC. Synthesis by CVD, however, hopes to realize patternable, highly crystalline graphene. It seems copper has emerged as the substrate of choice for graphene synthesis by CVD, and improvements in quality and post-processing in this fast-moving field will undoubtedly facilitate the development of many novel electronic and optoelectronic applications in the near future.

References

1. Ago H, Nakamura K, Ikeda K, Uehara N, Ishigami N and Tsuji M (2005), 'Aligned growth of isolated single-walled carbon nanotubes programmed by atomic arrangement of substrate surface', *Chem. Phys. Lett.*, 408, 433–438.
2. Ago H, Nishi T, Imamoto K, Ishigami N, Tsuji N, Ikuta T and Takahashi K (2010), 'Orthogonal growth of horizontally aligned single-walled carbon nanotube arrays', *J. Phys. Chem. C*, 114, 12925–12930.
3. Arnold M S, Stupp S I and Hersam M C (2005), 'Enrichment of single-walled carbon nanotubes by diameter in density gradients', *Nano Lett.*, 5, 713–718.
4. Arnold M S, Green A A, Hulvat J F, Stupp S I and Hersam M C (2006), 'Sorting carbon nanotubes by electronic structure using density differentiation', *Nature Nanotechnol.*, 1, 60–65.
5. Bae S, Kim H K, Lee Y B, Xu X F, Park J-S, Zheng Y, Balakrishnan J, Lei T, Kim H R, Song Y I, Kim Y-J, Kim K S, Özyilmaz B, Ahn J-H, Hong B H and Iijima S (2010), 'Roll-to-roll production of 30-inch graphene films for transparent electrodes', *Nature Nanotechnol.*, 5, 574–578.
6. Bandow S, Asaka S, Saito Y, Rao A M, Grigorian L, Richter E and Eklund P C (1998), 'Effect of the growth temperature on the diameter distribution and chirality of single-wall carbon nanotubes', *Phys. Rev. Lett.*, 80, 3779–3782.
7. Benedict L X, Louie S G and Cohen M L (1995), 'Static polarizabilities of single-wall carbon nanotubes', *Phys. Rev. B*, 52, 8541–8649.
8. Berger C, Song Z M, Li X B, Wu X S, Brown N, Naud C, Mayou D, Li T B, Hass J, Marchenkov A N, Conrad E H, First P N and de Heer W A (2006), 'Electronic confinement and coherence in patterned epitaxial graphene', *Science*, 312, 1191–1195.
9. Bethune D S, Kiang C H, DeVries M, Gorman G, Savoy R, Vasquez J and Beyers R (1993), 'Cobalt-catalysed growth of carbon nanotubes with single-atomic-layer walls', *Nature*, 363, 605–607.
10. Blake P, Hill E W, Castro Neto A H, Novoselov K S, Jiang D, Yang R, Booth T J and Geim K (2007), 'Making graphene visible', *Appl. Phys. Lett.*, 91, 063124.
11. Bronikowski M J, Willis P A, Colbert D T, Smith K A and Smalley R E (2001), 'Gas-phase production of carbon single-walled nanotubes from carbon monoxide via the HiPco process: A parametric study', *J. Vac. Sci. Technol. A*, 19, 1800–1805.
12. Cassell A M, Raymakers J A, Kong J and Dai H J (1999), 'Large scale CVD synthesis of single-walled carbon nanotubes', *J. Phys. Chem. B*, 103, 6484–6492.
13. Cançado L G, Takai K, Enoki T, Endo M, Kim Y A, Mizusaki H, Jorio A, Coelho L N, Magalhães-Paniago R and Pimenta M A (2006), 'General equation for the determination of the crystallite size L_a of nanographite by Raman spectroscopy', *Appl. Phys. Lett.*, 88, 163106.
14. Castro Neto A H, Guinea F, Peres N M R, Novoselov K S and Geim A K (2009), 'The electronic properties of graphene', *Rev. Mod. Phys.*, 81, 109–162.
15. Cheng H M, Li F, Su G, Pan H Y, He L L, Sun X and Dresselhaus M S (1998), 'Large-scale and low-cost synthesis of single-walled carbon nanotubes by the catalytic pyrolysis of hydrocarbons', *Appl. Phys. Lett.*, 72, 3282–3284.
16. Chiashi S, Okabe H, Inoue T, Shiomi J, Sato T, Kono S, Terasawa M and Maruyama S (2012), 'Growth of horizontally aligned single-walled carbon nanotubes on the singular R-plane (10−11) of quartz', *J. Phys. Chem. C*, 116, 6805–6808.
17. Coraux J, N'Diaye A T, Busse C and Michely T (2008), 'Structural coherency of

graphene on Ir(111)', *Nano Lett.*, 8, 565–570.
18. Dai H J, Rinzler A G, Nikolaev P, Thess A, Colbert D T and Smalley R E (1996), 'Single-wall nanotubes produced by metal-catalyzed disproportionation of carbon monoxide', *Chem. Phys. Lett.*, 260, 471–475.
19. Eda G and Chhowalla M (2010), 'Chemically derived graphene oxide: Towards large-area thin-film electronics and optoelectronics', *Adv. Mater.*, 22, 2392–2415.
20. Einarsson E, Shiozawa H, Kramberger C, Rümmeli M H, Grüneis A, Pichler T and Maruyama S (2007), 'Revealing the small-bundle internal structure of vertically aligned single-walled carbon nanotube films', *J. Phys. Chem. C*, 111, 17861–17864.
21. Eizenberg M and Blakely J M (1979), 'Carbon monolayer phase condensation on Ni(111)', *Surf. Sci.*, 82, 228–236.
22. Emtsev K V, Bostwick A, Horn K, Jobst J, Kellogg G L, Ley L, McChesney J L, Ohta T, Reshanov S A, Röhrl J, Rotenberg E, Schmid A K, Waldmann D, Weber H B and Seyller T (2009), 'Towards wafer-size graphene layers by atmospheric pressure graphitization of silicon carbide', *Nature Mater.*, 8, 203–207.
23. Endo M (1988), 'Grow carbon fibers in the vapor phase: What you can make out of these strong materials and how to make them', *Chemtech, Am. Chem. Soc.,* September 1988, 568–576.
24. Fernández-Morán H (1960), 'Improved pointed filaments of tungsten, rhenium, and tantalum for high-resolution electron microscopy and electron diffraction', *J. Appl. Phys.*, 31, 1840.
25. Ferrari A C, Meyer J C, Scardaci V, Casiraghi C, Lazzeri M, Mauri F, Piscanec S, Jiang D, Novoselov K S, Roth S and Geim A K (2006), 'Raman spectrum of graphene and graphene layers', *Phys. Rev. Lett.*, 97, 187401.
26. Furtado C A, Kim U J, Gutierrez H R, Pan L, Dickey E C and Eklund P C (2004), 'Debundling and dissolution of single-walled carbon nanotubes in amide solvents', *J. Am. Chem. Soc.*, 126, 6095–6105.
27. Futaba D N, Hata K, Yamada T, Mizuno K, Yumura M and Iijima S (2005), 'Kinetics of water-assisted single-walled carbon nanotube synthesis revealed by a time-evolution analysis', *Phys. Rev. Lett.*, 95, 056104.
28. Futaba D N, Hata K, Namai T, Yamada T, Mizuno K, Hayamizu Y, Yumura M and Iijima S (2006a), '84% catalyst activity of water-assisted growth of single walled carbon nanotube forest characterization by a statistical and macroscopic approach', *J. Phys. Chem. B*, 110, 8035–8038.
29. Futaba D N, Hata K, Yamada T, Hiraoka T, Hayamizu Y, Kakudate Y, Taniake O, Hatori H, Yumura M and Iijima S (2006b), 'Shape-engineerable and highly densely packed single-walled carbon nanotubes and their application as super-capacitor electrodes', *Nature Mater.*, 5, 987–994.
30. Futaba D N, Goto J, Yasuda S, Yamada T, Yumura M and Hata K (2009), 'General rules governing the highly efficient growth of carbon nanotubes', *Adv. Mater.*, 21, 4811–4815.
31. Gamo Y, Nagashima A, Wakabayashi M, Terai M and Oshima C (1997), 'Atomic structure of monolayer graphite formed on Ni(111)', *Surf. Sci.*, 374, 61–64.
32. Geim A K and MacDonald A H (2007), 'Graphene: Exploring carbon flatland', *Physics Today*, August 2007, 35–41.
33. Guo T, Nikolaev P, Thess A, Colbert D T and Smalley R E (1995), 'Catalytic growth of single-walled nanotubes by laser vaporization', *Chem. Phys. Lett.*, 243, 49–54.
34. Hafner J H, Bronikowski M J, Azamian B R, Nikolaev P, Rinzler A G, Colbert D T,

Smith K A and Smalley R E (1998), 'Catalytic growth of single-wall carbon nanotubes from metal particles', *Chem. Phys. Lett.*, 296, 195–202.
35. Han S, Liu X L and Zhou C W (2005), 'Template-free directional growth of single-walled carbon nanotubes on a- and r-plane sapphire', *J. Am. Chem. Soc.*, 127, 5294–5295.
36. Harutyunyan A R, Chen G G, Paronyan T M, Pigos E M, Kuznetsov O A, Hewaparakrama K, Kim S M, Zakharov D, Stach E A and Sumanasekera G U (2009), 'Preferential growth of single-walled carbon nanotubes with metallic conductivity', *Science*, 326, 116–120.
37. Hasegawa K and Noda S (2011), 'Millimeter-tall single-walled carbon nanotubes rapidly grown with and without water', *ACS Nano*, 5, 975–984.
38. Hass J, Varchon F, Millán-Otoya J E, Sprinkle M, Sharma N, de Heer W A, Berger C, First P N, Magaud L and Conrad E H (2008), 'Why multilayer graphene on 4*H*-SiC(000-1) behaves like a single sheet of graphene', *Phys. Rev. Lett.*, 100, 125504.
39. Hata K, Futaba D N, Mizuno K, Namai T, Yumura M and Iijima S (2004), 'Water-assisted highly efficient synthesis of impurity-free single-walled carbon nanotubes', *Science*, 306, 1362–1364.
40. Hayamizu Y, Yamada T, Mizuno K, Davis R C, Futaba D N, Yumura M and Hata K (2008), 'Integrated three-dimensional microelectromechanical devices from processable carbon nanotube wafers', *Nature Nanotechnol.*, 3, 289–294.
41. Hernandez Y, Nicolosi V, Lotya M, Blighe F M, Zun Z Y, De S, McGovern I T, Holland B, Byrne M, Gun'ko Y K, Boland J J, Niraj P, Duesberg G, Krishnamurthy S, Goodhue R, Hutchison J, Scardaci V, Ferrari A C and Coleman J N (2008), 'High-yield production of graphene by liquid-phase exfoliation of graphite', *Nature Nanotechnol.*, 3, 563–568.
42. Hiraoka T, Yamada T, Hata K, Futaba D N, Kurachi H, Uemura S, Yumura M and Iijima S (2006), 'Synthesis of single- and double-walled carbon nanotube forests on conducting metal foils', *J. Am. Chem. Soc.*, 128, 13338–13339.
43. Hofmann S, Sharma R, Ducati C, Du G H, Mattevi C, Cepek C, Cantoro M, Pisana S, Parvez A, Cervantes-Sodi F, Ferrari A C, Dunin-Borkowski R, Lizzit S, Petaccia L, Goldoni A and Robertson J (2007), 'In situ observations of catalyst dynamics during surface-bound carbon nanotube nucleation', *Nano Lett.*, 7, 602–608.
44. Hong S W, Banks T and Rogers J A (2010), 'Improved density in aligned arrays of single-walled carbon nanotubes by sequential chemical vapor deposition on quartz', *Adv. Mater.*, 22, 1826–1830.
45. Huang S M, Cai X Y and Liu J (2003), 'Growth of millimeter-long and horizontally aligned single-walled carbon nanotubes on flat substrates', *J. Am. Chem. Soc.*, 125, 5636–5637.
46. Hummers W S and Offeman R E, (1958), 'Preparation of graphitic oxide', *J. Am. Chem. Soc.*, 80, 1339.
47. Iijima S and Ichihashi T, (1993), 'Single-shell carbon nanotubes of 1-nm diameter', *Nature*, 363, 603–605.
48. Ismach A, Kantorovich D and Joselevich E (2005), 'Carbon nanotube graphoepitaxy: Highly oriented growth by faceted nanosteps', *J. Am. Chem. Soc.*, 127, 11554–11555.
49. Jiao L Y, Zhang L, Wang X R, Diankov G and Dai H J (2009), 'Narrow graphene nanoribbons from carbon nanotubes', *Nature,* 458, 877–880.
50. Joselevich E and Lieber C M (2002), 'Vectorial growth of metallic and

semiconducting single-wall carbon nanotubes', *Nano Lett.*, 2, 1137–1141.
51. Journet C, Maser W K, Bernier P, Loiseau A, Lamy de la Chapelle M, Lefrant S, Deniard , Lee R and Fischer J E (1997), 'Large-scale production of single-walled carbon nanotubes by the electric-arc technique', *Nature*, 388, 756–758.
52. Kakehi K, Noda S, Maruyama S and Yamaguchi Y (2008), 'Growth valley dividing single- and multi-walled carbon nanotubes: Combinatorial study of nominal thickness of Co catalyst', *Jpn. J. Appl. Phys.*, 47, 1961–1965.
53. Kataura H, Kumazawa Y, Maniwa Y, Umezu I, Suzuki S, Ohtsuka Y and Achiba Y (1999), 'Optical properties of single-walled carbon nanotubes', *Synth. Met.*, 103, 2555–2558.
54. Kataura H, Kumazawa Y, Maniwa Y, Ohtsuka Y, Sen R, Suzuki S and Achiba Y (2000), 'Diameter control of single-walled carbon nanotubes', *Carbon*, 38, 1691–1697.
55. Kim J M, Cote L J, Kim F and Huang J X (2010), 'Visualizing graphene based sheets by fluorescence quenching microscopy', *J. Am. Chem. Soc.*, 132, 260–267.
56. Kim K S, Zhao Y, Jang H, Lee S Y, Kim J M, Kim K S, Ahn J-H, Kim P, Choi J-Y and Hong B H (2009), 'Large-scale pattern growth of graphene films for stretchable transparent electrodes', *Nature*, 457, 706–710.
57. Kitiyanan B, Alvarez W E, Harwell J H and Resasco D E (2000), 'Controlled production of single-wall carbon nanotubes by catalytic decomposition of CO on bimetallic Co–Mo catalysts', *Chem. Phys. Lett.*, 317, 497–503.
58. Kocabas C, Hur S-H, Gaur A, Meitl M A, Shim M and Rogers J A (2005), 'Guided growth of large-scale, horizontally aligned arrays of single-walled carbon nanotubes and their use in thin-film transistors', *Small*, 1, 1110–1116.
59. Kong J, Cassell A M and Dai H J (1998a), 'Chemical vapor deposition of methane for single-walled carbon nanotubes', *Chem. Phys. Lett.*, 292, 567–574.
60. Kong J, Soh K T, Cassell A M, Quate C F and Dai H J (1998b), 'Synthesis of individual single-walled carbon nanotubes on patterned silicon wafers', *Nature*, 395, 878–881.
61. Kosynkin D V, Higginbotham A L, Sinitskii A, Lomeda J R, Dimiev A, Price B K and Tour J M (2009), 'Longitudinal unzipping of carbon nanotubes to form graphene nanoribbons' *Nature*, 458, 872–877.
62. Kramberger C, Hambach R, Giorgetti C, Rümmeli M H, Knupfer M, Fink J, Büchner B, Reining L, Einarsson E, Maruyama S, Sottile F, Hannewald K, Olevano V, Marinopoulos A G and Pichler T (2008), 'Linear plasmon dispersion in single-wall carbon nanotubes and the collective excitation spectrum of graphene', *Phys. Rev. Lett.*, 100, 196803.
63. Krätschmer W, Fostiropoulos K and Huffman D R (1990), 'The infrared and ultraviolet absorption spectra of laboratory-produced carbon dust: Evidence for the presence of the C_{60} molecule', *Chem. Phys. Lett.*, 170, 167–170.
64. Kroto H W, Heath J R, O'Brien S C, Curl R F and Smalley R E (1985), 'C_{60}: Buckminsterfullerene', *Nature*, 318, 162–163.
65. Kroto H W and McKay K (1988), 'The formation of quasi-icosahedral spiral shell carbon particles', *Nature*, 331, 328–331.
66. Li X L, Wang X R, Zhang L, Lee S and Dai H J (2008), 'Chemically derived, ultrasmooth graphene nanoribbon semiconductors', *Science*, 319, 1229–1232.
67. Li X S, Cai W W, An J H, Kim S, Nah J, Yang D X, Piner R, Velamakanni A, Jung I, Tutuc E, Banjeree S K, Colombo L and Ruoff R S (2009a), 'Large-area synthesis of

high-quality and uniform graphene films on copper foils' *Science*, 324, 1312–1314.
68. Li X S, Cai W W, Colombo L and Ruoff R S (2009b), 'Evolution of graphene growth on Ni and Cu by carbon isotope labeling', *Nano Lett.*, 9, 4268–4272.
69. Li X S, Magnuson C W, Venugopal A, Tromp R M, Hannon J B, Vogel E M, Colombo L and Ruoff R S (2011), 'Large-Area Graphene Single Crystals Grown by Low-Pressure Chemical Vapor Deposition of Methane on Copper', *J. Am. Chem. Soc.*, 133, 2816–2819.
70. Li Y M, Mann D, Rolandi M, Kim W, Ural A, Hung S, Javey A, Cao J, Wang D W, Yenilmez E, Wang Q, Gibbons J F, Nishi Y and Dai H J (2004), 'Preferential growth of semiconducting single-walled carbon nanotubes by a plasma enhanced CVD method', *Nano Lett.*, 4, 317–321.
71. Lim G-K, Chen Z-L, Clark J, Goh R G S, Ng W-H, Tan H-W, Friend R H, Ho P K H and Chua L-L (2011), 'Giant broadband nonlinear optical absorption response in dispersed graphene single sheets', *Nature Photonics*, 5, 554–560.
72. Lin Y-M, Valdes-Garcia A, Han S-J, Farmer D B, Meric I, Sun Y, Wu Y Q, Dimitrakopoulos C, Grill A, Avouris Ph and Jenkins K A (2011), 'Wafer-scale graphene integrated circuit', *Science*, 332, 1294–1297.
73. Liu H P, Nishide D, Tanaka T and Kataura H (2011), 'Large-scale single-chirality separation of single-wall carbon nanotubes by simple gel chromatography', *Nature Commun.*, 2, 309.
74. Loh K P, Bao Q L, Eda G and Chhowalla M (2011), 'Graphene oxide as a chemically tunable platform for optical applications', *Nature Chem*, 2, 1015–1024.
75. Lopes dos Santos J M B, Peres N M R and Castro Neto A H (2007), 'Graphene bilayer with a twist: Electronic structure', *Phys. Rev. Lett.*, 99, 256802.
76. Lu X K, Yu M F, Huang H and Ruoff R S (1999), 'Tailoring graphite with the goal of achieving single sheets', *Nanotechnology*, 10, 269–272.
77. MacDonald A H and Bistritzer R (2011), 'Materials science: Graphene moiré mystery solved?', *Nature*, 474, 453–454.
78. Maruyama S, Kojima R, Miyauchi Y, Chiashi S and Kohno M (2002), 'Low-temperature synthesis of high-purity single-walled carbon nanotubes from alcohol' *Chem. Phys. Lett.*, 360, 229–234.
79. Miyata Y, Maniwa Y and Kataura H (2006), 'Selective oxidation of semiconducting single-wall carbon nanotubes by hydrogen peroxide', *J. Phys. Chem. B*, 110, 25–29.
80. Mukhopadhyay K, Koshio A, Sugai T, Tanaka N, Shinohara H, Konya Z and Nagy J B (1999), 'Bulk production of quasi-aligned carbon nanotube bundles by the catalytic chemical vapour deposition (CCVD) method', *Chem. Phys. Lett.*, 303, 117–124.
81. Murakami Y, Miyauchi Y, Chiashi S and Maruyama S (2003), 'Direct synthesis of high-quality single-walled carbon nanotubes on silicon and quartz substrates', *Chem. Phys. Lett.*, 377, 49–54.
82. Murakami Y, Chiashi S, Miyauchi Y, Hu M H, Ogura M, Okubo T and Maruyama S (2004), 'Growth of vertically aligned single-walled carbon nanotube films on quartz substrates and their optical anisotropy', *Chem. Phys. Lett.*, 385, 298–303.
83. Murakami Y and Maruyama S (2006), 'Detachment of vertically aligned single-walled carbon nanotube films from substrates and their re-attachment to arbitrary surfaces', *Chem. Phys. Lett.*, 422, 575–580.
84. Murata Y, Starodub E, Kappes B B, Ciobanu C V, Bartelt N C, McCarthy K F and Kodambaka S (2010), 'Orientation-dependent work function of graphene on Pd(111)', *Appl. Phys. Lett.*, 97, 143114.

85. Nakada K, Fujita M, Dresselhaus G and Dresselhaus M S (1996), 'Edge state in graphene ribbons: Nanometer size effect and edge shape dependence', *Phys. Rev. B*, 54, 17954–17961.
86. Ni Z H, Wang Y Y, Yu T, You Y M and Shen Z X (2008), 'Reduction of Fermi velocity in folded graphene observed by resonance Raman spectroscopy', *Phys. Rev. B*, 77, 235403.
87. Nikolaev P, Bronikowski M J, Bradley R K, Rohmund F, Colbert D T, Smith K A and Smalley R E (1999), 'Gas-phase catalytic growth of single-walled carbon nanotubes from carbon monoxide', *Chem. Phys. Lett.*, 313, 91–97.
88. Nishino H, Yasuda S, Namai T, Futaba D N, Yamada T, Yumura M, Iijima S and Hata K (2007), 'Water-assisted and highly efficient synthesis of single-walled carbon nanotubes forests from colloid nanoparticle catalysts', *J. Phys. Chem. C*, 111, 17961–17965.
89. Noda S, Hasegawa K, Sugime H, Kakehi K, Zhang Z, Maruyama S and Yamaguchi Y (2007), 'Millimeter-thick single-walled carbon nanotube forests: Hidden role of catalyst support', *Jpn. J. Appl. Phys.*, 46, L399–L401.
90. Novoselov K S, Geim A K, Morozov S V, Jiang D, Zhang Y, Dubonos S V, Grigorieva I V and Firsov A A (2004), 'Electric field effect in atomically thin carbon films', *Science*, 306, 666–669.
91. Novoselov K S, Jiang D, Schedin F, Booth T J, Khotkevich V V, Morozov S V and Geim A K (2005), 'Two-dimensional atomic crystals', *Proc. Nat. Acad. Sci.*, 102, 10451–10453.
92. Odahara G, Otani S, Oshima C, Suzuki M, Yasue T and Koshikawa Y (2011), 'In-situ observation of graphene growth on Ni(111)', *Surf. Sci.*, 605, 1095–1098.
93. Park S J and Ruoff R S (2009), 'Chemical methods for the production of graphenes', *Nature Nanotechnol*., 4, 217–224.
94. Pimenta M A, Dresselhaus G, Dresselhaus M S, Cançado L G, Jorio A and Saito R (2007), 'Studying disorder in graphite-based systems by Raman spectroscopy', *Phys. Chem. Chem. Phys.*, 9, 1276–1291.
95. Pint C L, Xu Y-Q, Pasquali M and Hauge R H (2008), 'Formation of highly dense aligned ribbons and transparent films of single-walled carbon nanotubes directly from carpets', *ACS Nano*, 2, 1871–1878.
96. Qu L T, Du F and Dai L M (2008), 'Preferential syntheses of semiconducting vertically aligned single-walled carbon nanotubes for direct use in FETs', *Nano Lett.*, 8, 2682–2687.
97. Reina A, Jia X T, Ho J, Nezich D, Son H B, Bulovic V, Dresselhaus M S and Kong J (2009), 'Large area, few-layer graphene films on arbitrary substrates by chemical vapor deposition', *Nano Lett.*, 9, 30–35.
98. Riggs J E, Walker D B, Carroll D L and Sun Y-P (2000), 'Optical limiting properties of suspended and solubilized carbon nanotubes', *J. Phys. Chem. B*, 104, 7071–7076.
99. Robertson D H, Brenner D W and White C T (1992), 'On the way to fullerenes: Molecular dynamics study of the curling and closure of graphitic ribbons', *J. Phys. Chem.*, 96, 6133–6135.
100. Satishkumar B C, Govindaraj A, Sen R and Rao C N R (1998), 'Single-walled nanotubes by the pyrolysis of acetylene-organometallic mixtures', *Chem. Phys. Lett.*, 293, 47–52.
101. Schniepp H C, McAllister M J, Sai H, Herrera-Alonso M, Adamson D H, Prud'homme R K, Car R, Saville D A and Aksay I A (2006), 'Functionalized single

graphene sheets derived from splitting graphite oxide', *J. Phys. Chem. B*, 110, 8535–8539.
102. Shelton J C, Patil H R and Blakely J M (1974), 'Equilibrium segregation of carbon to a nickel(111) surface: A surface phase transition', *Surf. Sci.*, 43, 493–520.
103. Shi Z J, Lian Y F, Zhou X H, Gu Z N, Zhang Y G, Iijima S, Zhou L X, Yue K T and Zhang S L (1999), 'Mass-production of single-wall carbon nanotubes by arc discharge method', *Carbon*, 37, 1449–1453.
104. Song Y-W, Einarsson E, Yamashita S and Maruyama S (2007), 'All-fiber pulsed lasers passively mode-locked by transferable vertically aligned carbon nanotube film', *Opt. Lett.*, 32, 1399–1401.
105. Sprinkle M, Ruan M, Hu Y, Hankinson J, Rubio-Roy M, Zhang B, Wu X, Berger C and de Heer W A (2010), 'Scalable templated growth of graphene nanoribbons on SiC', *Nature Nanotechnol.*, 5, 727–731.
106. Stankovich S, Dikin D A, Piner R D, Kohlhaas K A, Kleinhammes A, Jia Y Y, Wu Y, Nguyen S B T and Ruoff R S (2007), 'Synthesis of graphene-based nanosheets via chemical reduction of exfoliated graphite oxide', *Carbon*, 45, 1558–1565.
107. Sun Z Z, Yan Z, Yao J, Beitler E, Zhu Y and Tour J M (2010), 'Growth of graphene from solid carbon sources', *Nature*, 468, 549–552.
108. Sutter P W, Flege J-I and Sutter E A (2008), 'Epitaxial graphene on ruthenium', *Nature Mater.*, 7, 406–411.
109. Sutter P, Sadowski J T and Sutter E (2009), 'Graphene on Pt(111): Growth and substrate interaction', *Phys. Rev. B*, 80, 245411.
110. Takahashi K, Yamada K, Kato H, Hibino H and Homma Y (2012), 'In situ scanning electron microscopy of graphene growth on polycrystalline Ni substrate', *Surf. Sci.*, 606, 728–732.
111. Thess A, Lee R, Nikolaev P, Dai H J, Petit P, Robert J, Xu C H, Lee Y H, Kim S G, Rinzler A G, Colbert D T, Scuseria G E, Tománek D, Fischer J E and Smalley R E (1996), 'Crystalline ropes of metallic carbon nanotubes', *Science*, 273, 483–487.
112. Thurakitseree T, Einarsson E, Xiang R, Zhao P, Aikawa S, Chiashi S, Shiomi J and Maruyama S (2012a), 'Diameter controlled chemical vapor deposition synthesis of single-walled carbon nanotubes', *J. Nanosci. Nanotechnol.*, 12, 370–376.
113. Thurakitseree T, Kramberger C, Zhao P, Aikawa S, Harish S, Chiashi S, Einarsson E and Maruyama S (2012b), 'Diameter-controlled and nitrogen-doped vertically aligned single-walled carbon nanotubes', *Carbon*, 50, 2635–2640.
114. Tu X M, Manohar S, Jagota A and Zheng M (2009), 'DNA sequence motifs for structure-specific recognition and separation of carbon nanotubes', *Nature,* 460, 250–253.
115. Vallés C, Drummond C, Saadaoui H, Furtado C A, He M S, Roubeau O, Ortolani L, Monthioux and Pénicaud A (2008), 'Solutions of negatively charged graphene sheets and ribbons', *J. Am. Chem. Soc.*, 130, 15802–15804.
116. Weatherup R S, Bayer B C, Blume R, Ducati C, Baehtz C, Schlögl R and Hofmann S (2011), 'In situ characterization of alloy catalysts for low-temperature graphene growth', *Nano Lett.*, 11, 4154–4160.
117. Xiang R, Einarsson E, Murakami Y, Shiomi J, Chiashi S, Tang Z K and Maruyama S (2012), 'Diameter modulation of vertically aligned single-walled carbon nanotubes', *ACS Nano*, 6, 7472–7479.
118. Yan Z, Lin J, Peng Z W, Sun Z Z, Zhu Y, Li L, Xiang C S, Samuel E L, Kittrell C and Tour J M (2012), 'Toward the synthesis of wafer-scale single-crystal graphene on

copper foils', *ACS Nano*, Article ASAP, Available from http://pubs.acs.org/doi/abs/10.1021/nn303352k [02 Oct 2012].
119. Zhang G Y, Mann D, Zhang L, Javey A, Li Y M, Yenilmez E, Wang Q, McVittie J P, Nishi Y, Gibbons J and Dai H J (2005), 'Ultra-high-yield growth of vertical single-walled carbon nanotubes: Hidden roles of hydrogen and oxygen', *Proc. Nat. Acad. Sci.*, 102, 16141–16145.
120. Zhang G Y, Qi P F, Wang X R, Lu Y R, Li X L, Tu R, Bangsaruntip S, Mann D, Zhang L and Dai H J (2006), 'Selective etching of metallic carbon nanotubes by gas-phase reaction', *Science*, 314, 974–977.
121. Zhang Y, Gomez L, Ishikawa F N, Madaria A, Ryu K, Wang C, Badmaev A and Zhou C W (2011), 'Comparison of graphene growth on single-crystalline and polycrystalline Ni by chemical vapor deposition', *J. Phys. Chem. Lett.*, 1, 3101–3107.
122. Zhang Y B, Small J P, Pontius W V and Kim P (2005), 'Fabrication and electric-field-dependent transport measurements of mesoscopic graphite devices', *Appl. Phys. Lett.*, 86, 073104.
123. Zhang Y G, Chang A, Cao J, Wang Q, Kim W, Li Y M, Morris N, Yenilmez E, Kong J and Dai H J (2001), 'Electric-field-directed growth of aligned single-walled carbon nanotubes', *Appl. Phys. Lett.*, 79, 3155–3157.
124. Zhao P, Einarsson E, Xiang R, Murakami Y and Maruyama S (2010), 'Controllable expansion of single-walled carbon nanotube dispersions using density gradient ultracentrifugation', *J. Phys. Chem. C*, 114, 4831–4834.
125. Zhao X, Wang M, Ohkohchi M and Ando Y (1996), *Bull. Res. Inst. Meijo Univ.*, 1, 7.
126. Zheng M, Jagota A, Semke E D, Diner B A, Mclean R S, Lustig S R, Richardson R E and Tassi N G (2003), 'DNA-assisted dispersion and separation of carbon nanotubes', *Nature Mater.*, 2, 338–342.
127. Zhou W W, Han Z Y, Wang J Y, Zhang Y, Jin Z, Sun X, Zhang Y W, Yan C H and Li Y (2006), 'Copper catalyzing growth of single-walled carbon nanotubes on substrates', *Nano Lett.*, 6, 2897–2990.

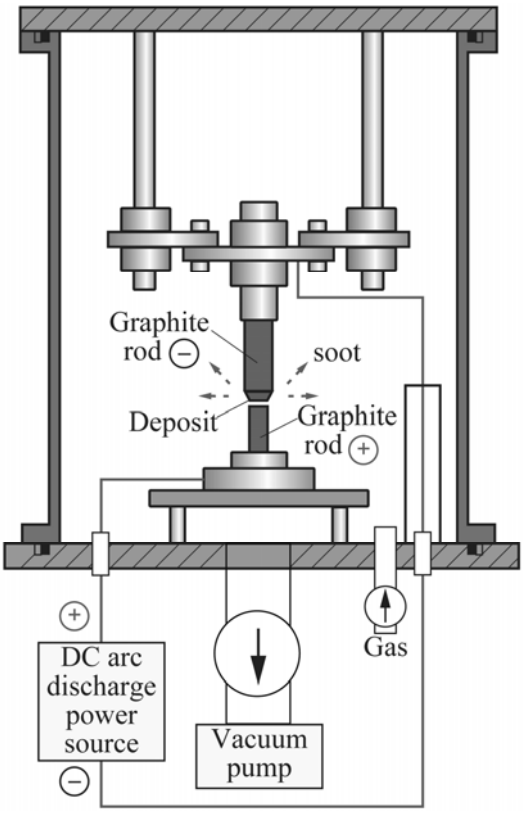

Figure 2.1
Schematic of the apparatus used to synthesize SWNTs by the arc-discharge method. Fullerenes are formed in the soot, and SWNTs can be nucleated by adding a small amount of metal in the negative electrode. Adapted with permission from X. Zhao *et al.* (1996). Copyright 1996, Meijo University.

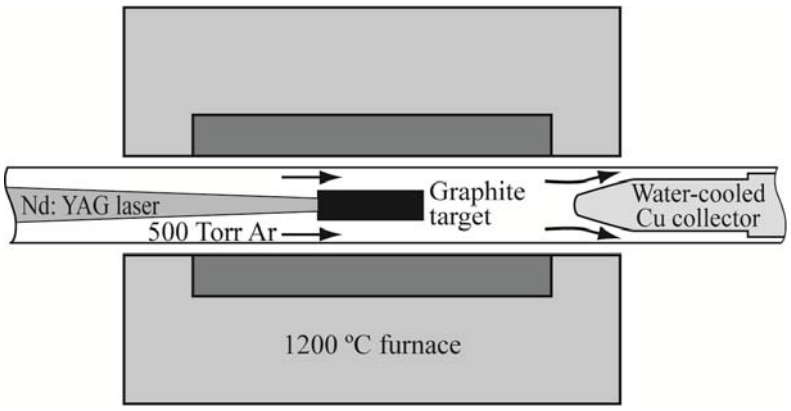

Figure 2.2
Schematic of the apparatus used to synthesize SWNTs by the laser ablation method. A graphite target containing a few atomic per cent of transition metal sits inside an electric furnace. SWNTs are synthesized by ablating the target with a pulsed laser under flowing argon. SWNTs are collected on a cooled piece of copper located downstream. Reprinted from Guo *et al.* (1995) with permission from Elsevier (recreated for clarity).

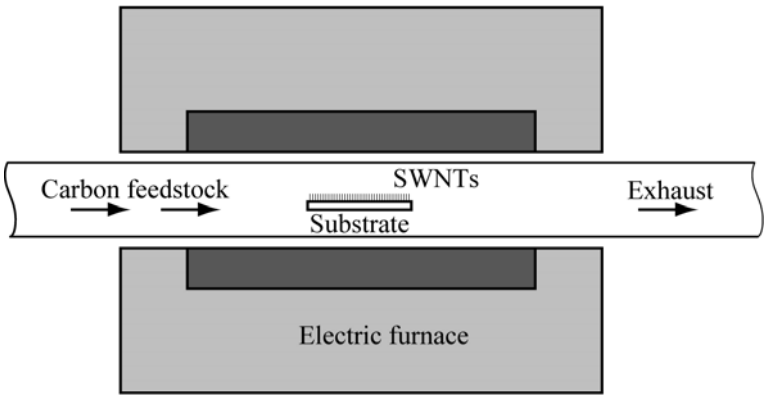

Figure 2.3
Simplified schematic showing a CVD system in which the catalyst is supported by a substrate. Various carbon-containing precursors can be used to synthesize SWNTs under a wide range of temperatures and pressures.

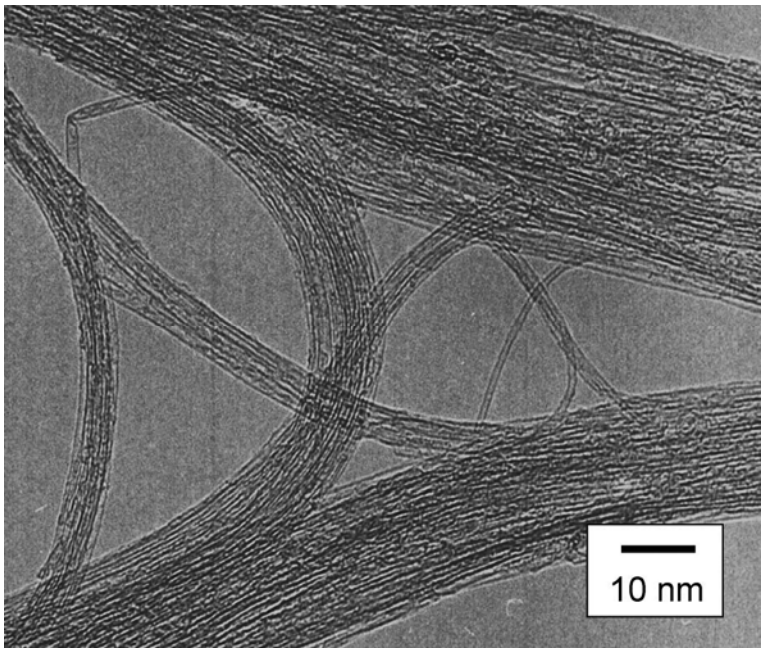

Figure 2.4
Transmission electron micrograph showing the clean, high-quality SWNTs synthesized from ethanol vapor. Reprinted from Maruyama *et al.* (2002) with permission from Elsevier.

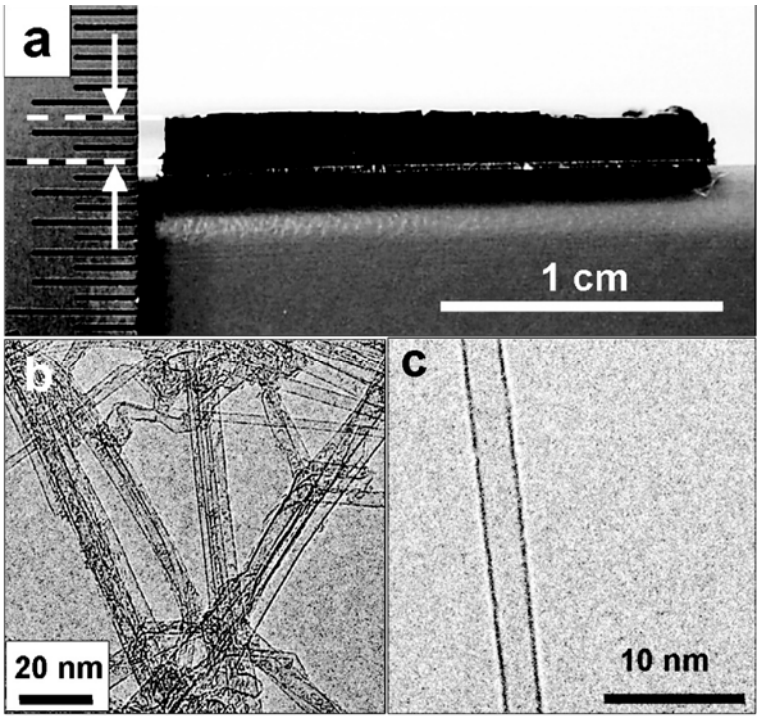

Figure 2.5
(a) Photograph of 1.5 mm nanotube forest synthesized by the water-assisted CVD method. (b) Low-resolution and (c) high-resolution TEM micrographs of the SWNTs. Adapted with permission from Nishino *et al.* (2007), *J. Phys. Chem. C* 111, 17961–17965. Copyright 2007, American Chemical Society.

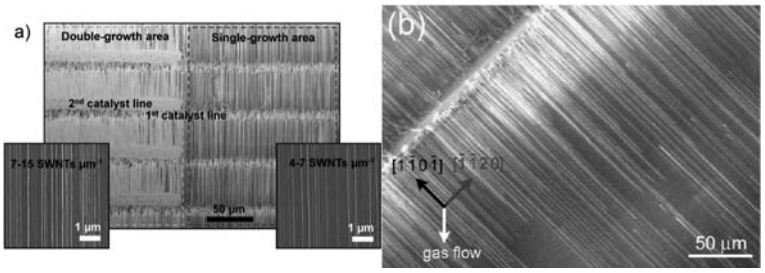

Figure 2.6
Scanning electron micrographs showing aligned SWNTs synthesized on (a) crystal quartz, and (b) sapphire substrates. (a) is reprinted with permission from Hong *et al.* (2010). Copyright 2010, Wiley-Blackwell. (b) is reprinted with permission from Ago *et al.* (2010), *J. Phys. Chem. C* 114, 12925–12930. Copyright 2010, American Chemical Society.

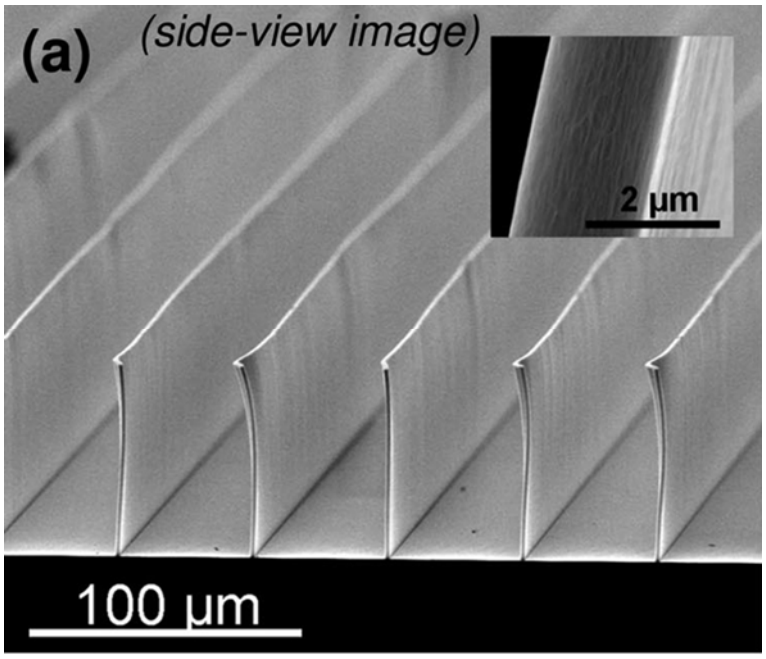

Figure 2.7
Scanning electron micrograph showing an array of SWNTs patterned into thin walls. Inset shows a higher magnification image of the wall. Reprinted with permission from Pint *et al.* (2008), *ACS Nano* 2, 1871–1878. Copyright 2008, American Chemical Society.

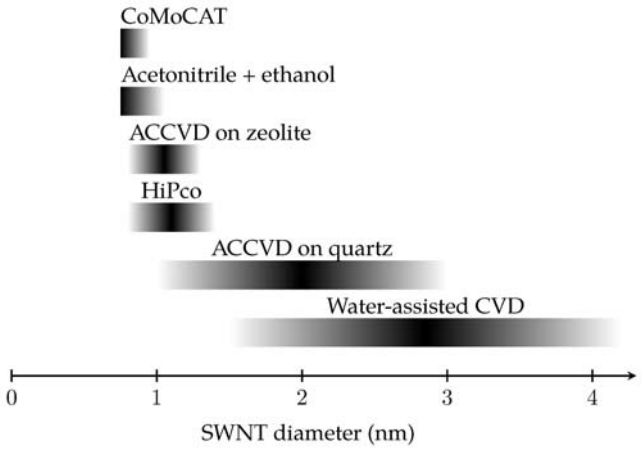

Figure 2.8
Approximate diameter ranges for SWNTs produced by various methods.

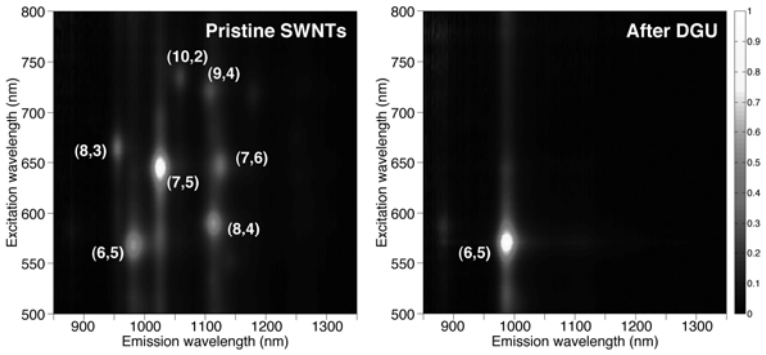

Figure 2.9
Photoluminescence excitation map of dispersed pristine SWNTs (left) and (6,5) SWNTs selectively extracted by density gradient ultracentrifugation (right). Adapted with permission from P. Zhao *et al.* (2010), *J. Phys. Chem. C* 114, 4831–4834. Copyright 2010, American Chemical Society.

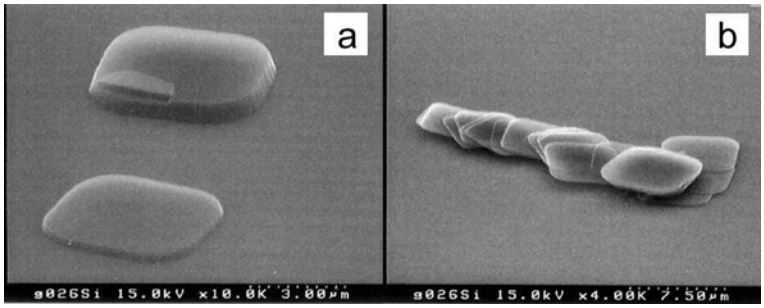

Fig 2.10
Scanning electron micrographs of (a) a thin graphite flake next to an HOPG island on a Si(001) surface, and (b) several thin flakes sheared off from one HOPG island. Reprinted with permission from Lu *et al.* (1999), *Nanotechnology* 10, 269–272. Copyright 1999, IOP Publishing.

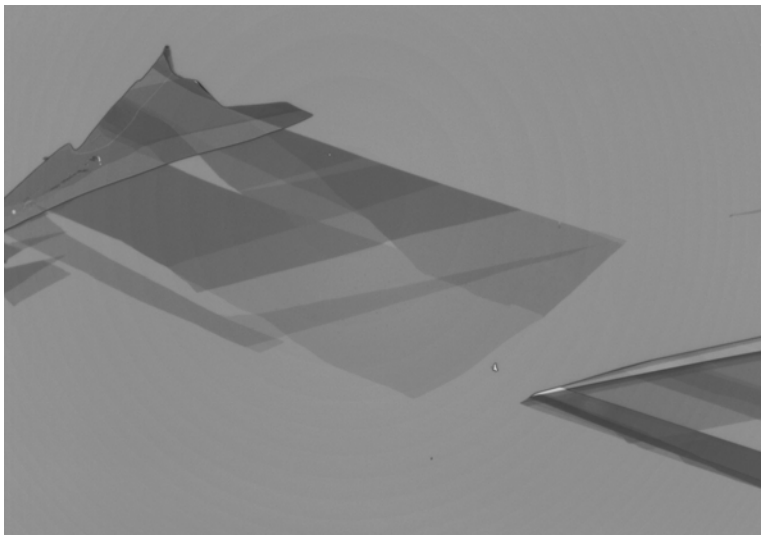

Figure 2.11
Optical image of graphene sitting atop a silicon wafer with 300 nm silicon oxide layer. A single layer is visible near the center of the image, and overlapping layers considerably darken the appearance. Adapted with permission from the University of Manchester. Copyright 2012, the University of Manchester.

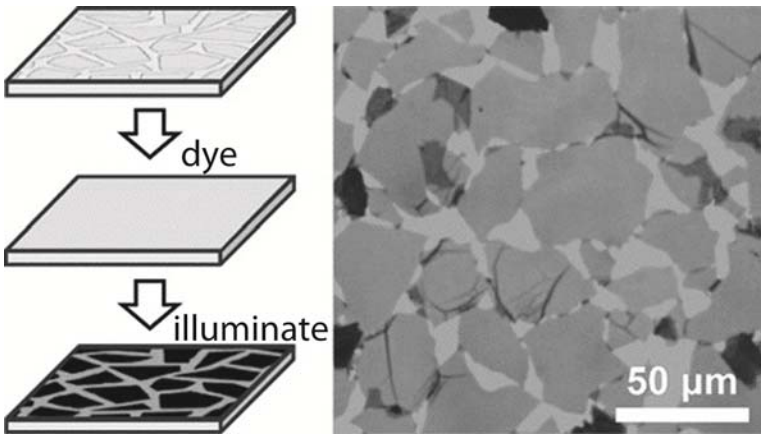

Figure 2.12
Left: preparation of graphene oxide flakes for imaging by fluorescence quenching microscopy. Right: optical image of graphene oxide flakes visibly enhanced by a removable dye coating. Adapted with permission from J.M. Kim *et al.* (2010), *J. Am. Chem. Soc.* 132, 260–267. Copyright 2010, American Chemical Society.

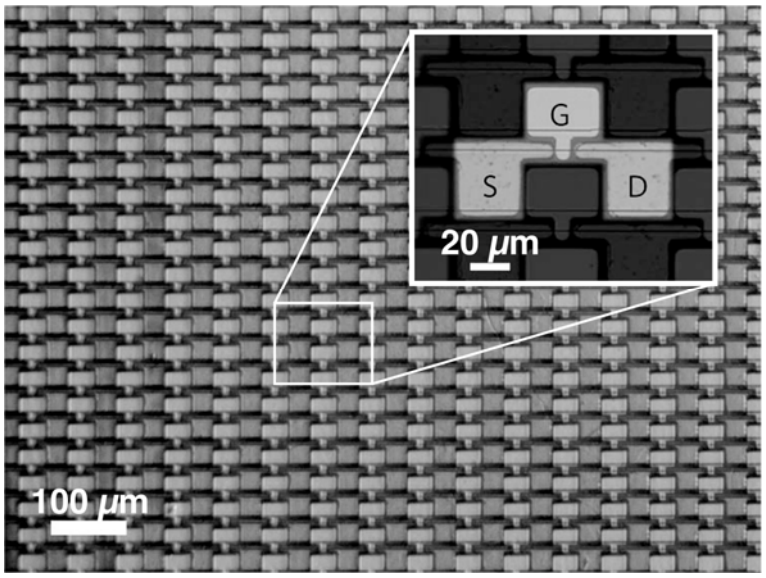

Figure 2.13
Optical micrograph of graphene transistor array obtained by patterned synthesis on SiC. Inset shows the source (S), drain (D), and gate (G) electrodes. Channel length is 7 μm, and density is 40,000 devices per cm^2. Adapted with permission from Macmillan Publishers Ltd: *Nature Nanotechnol.* 5: 727–731, copyright 2010.

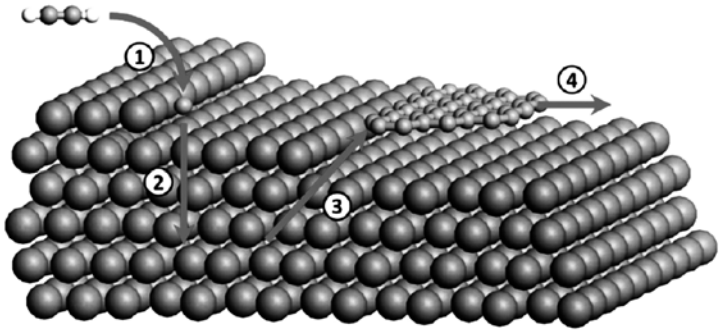

Figure 2.14
Graphene growth mechanism proposed by Hofmann and co-workers in which the precursor (1) dissociates, (2) diffuses through the Ni, (3) re-emerges at a step edge, and (4) extends the sp^2 graphene network. Reprinted with permission from Weatherup *et al.* (2011), *Nano Lett.* 11, 4154–4160. Copyright 2011, American Chemical Society.

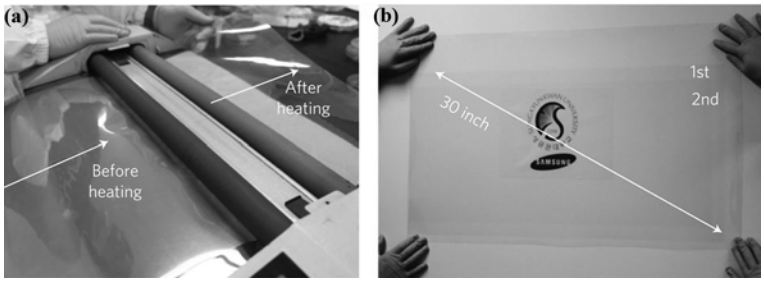

Figure 2.15
(a) Roll-to-roll process by which CVD-grown graphene is transferred onto a transparent polymer sheet. (b) A 30-inch (76 cm) graphene film after transfer. Adapted with permission from Macmillan Publishers Ltd: *Nature Nanotechnol.* 5: 574–578, copyright 2010.

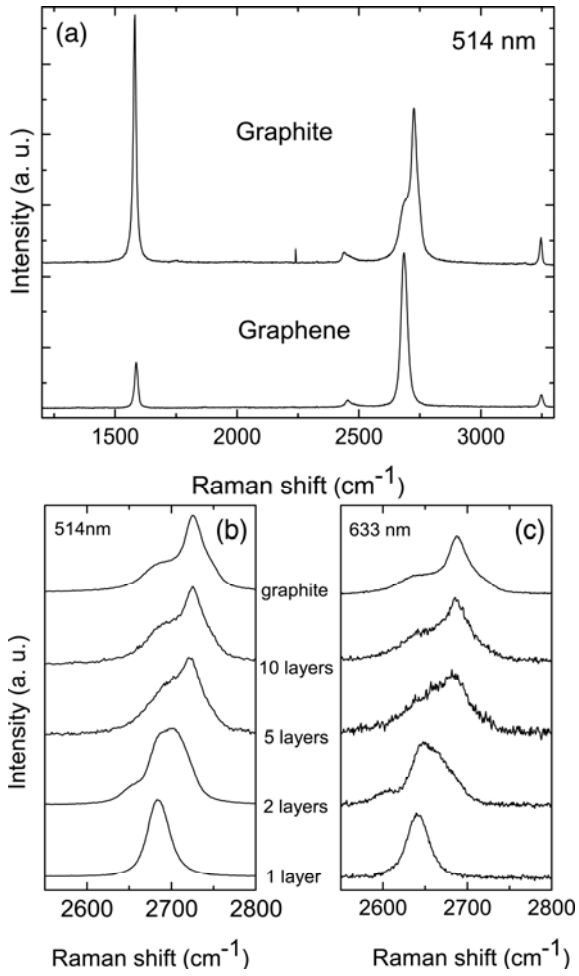

Figure 2.16
(a) Comparison of Raman spectra for bulk graphite and graphene at 514 nm excitation. Spectra have been scaled to have similar 2D peak intensities (at ~2700 cm^{-1}). (b,c) Evolution of the 2D feature with layer number for (b) 514 nm and (c) 633 nm excitation. Reprinted with permission from Ferrari *et al.* (2006) *Phys. Rev. Lett.* 97, 187401. Copyright 2006 by the American Physical Society.